

## Numerical simulation of heat conduction for the growth of anisotropic layered GaSe crystals

E. Tasarkuyu\*<sup>1</sup> and B. G. Akinoglu<sup>2</sup>

<sup>1</sup> Physics Department, Mugla University, Mugla, Turkey

<sup>2</sup> Physics Department, Middle East Technical University, Ankara, Turkey

Received 5 December 2003, revised 13 February 2004, accepted 26 March 2004

Published online 1 August 2004

**Key words** Bridgman technique, heat transfer in anisotropic media, 3D numerical simulation, GaSe.

**PACS** 81.10.Aj

In this report, we present the usage of a second rank cylindrical conductivity tensor which we derived to simulate the crystal growth processes of a layered compound GaSe in a cylindrical enclosure by directional solidification. Use of such a tensor is inevitable in the simulations of the growth of highly anisotropic crystals having layered structure, since the crystallographic orientation of the grown material is not necessarily aligned with the ampoule symmetry. Using the finite difference control volume approach in 3D, we solved transient heat conduction equation for a highly anisotropic solid in a cylindrical enclosure. We obtained sloped thermal fields and isothermal surfaces and the magnitudes of the slopes are strong functions of both azimuthal angle and growth orientation. The results showed that the orientation of the crystallographic axes of GaSe in the enclosure is quite effective in the steady and the transient fields, isotherms, and axial and radial temperature gradient within the material. Increase of Bi number decreases the magnitude of the slope of isothermal surface. Anisotropy of the conductivity seems to be effective in the orientation of the growth direction of the resulting crystal within the cylindrical ampoule.

© 2004 WILEY-VCH Verlag GmbH & Co. KGaA, Weinheim

### 1 Introduction

The increasing applications of semiconductor based electronics and optoelectronics generate a massive demand for high quality semiconductor single crystals. This demand is mainly supplied by the crystals produced from melt using special techniques by characterized control of the liquid-solid phase transition [1]. The most important techniques are crystal pulling out of a crucible (Czochralski-method) [2], solidification by a free floatzone [3] and Bridgman-Stockberger techniques [4].

It is believed that the macroscopic solid-liquid (SL) interface shape strongly influences the quality of the crystals grown by these techniques. Highly curved interfaces are likely to result unwanted inhomogeneous growth, and generation and propagation of defects during the growth [5]. If the crystal is grown with a flat interface shape, then it grows with minimal thermal stress, because the thermal changes are in the direction of growth [6]. Since the thermal stresses are reduced at the interface, the grown crystal exhibits very low dislocation densities. On the other hand, concave (with respect to solid) interface shape leads to increased nucleation at the ampoule wall compared to the central region, hence the greater possibility of polycrystalline growth. Therefore, start of growth at the wall should be prevented by making the growth face slightly convex [6,7].

Finding the means of controlling the solidification interface could yield the growth of defect free crystals. In order to determine the macroscopic solid-liquid (SL) interface shape researchers have been investigating the effects of different parameters involved in the crystal growth process. Their investigations rely mostly on the

\* Corresponding author: e-mail: tergun@metu.edu.tr

numerical simulations as well as the theoretical calculations. Many factors have been shown to be effective but the thermal conductivity ratio of liquid and solid phases of a grown material has been shown to determine the heat transfer rate and especially the direction of the heat flux near the interface [8,9,10]. The liquid-solid conductivity ratio  $k_l / k_s$  determines the shape and the position of the interface [8]. On the other hand, the effective heat exchange between the furnace and the ampoule depends on the  $k_a / k_s$  and  $k_a / k_l$  ratios [11]. Barat et al. [12] indicated that the interface curvature is a result of the local heat exchange between the ampoule and the material. The direction and the intensity of thermal convection in the melt is also affected by the radial temperature gradient which is in turn affected by the differences of ampoule-melt-solid conductivities [13].

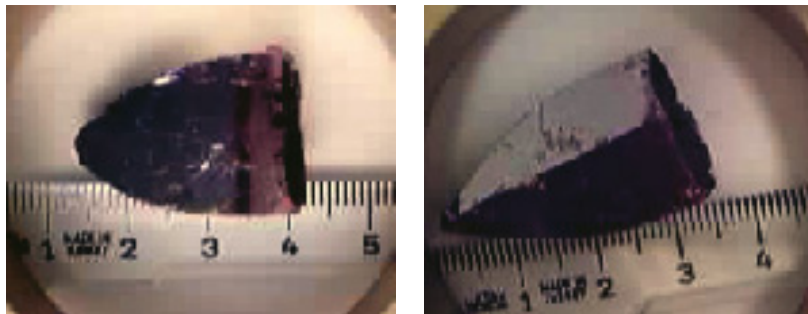


Fig. 1 GaSe crystal ingots grown in our laboratory with layers parallel to the ampoule axis.

The mismatch in the thermal conductivities of the melt-solid-ampoule system becomes a greater problem when the grown material has anisotropic thermal conductivity. This is indeed the case for many layered compounds such as GaSe that we grow in our laboratory by Bridgman technique. Because of the difficulty of obtaining analytical or numerical solutions to heat conduction problems in anisotropic media some investigators examined the effect of anisotropic conductivity only for orthotropic cases, namely, only the diagonal elements of the conductivity tensor exist [9,14,15]. In ref. [14], it is stated that GaSe crystals are usually grown with the  $c$ -axis parallel to the ampoule axis so that a diagonal tensor which contains two different constant conductivity values for the  $z$  and the  $r$  directions can be used in the heat conduction equation. Lee and Pearlstein in [15] calculated the deviations of axially asymmetric tensor elements in 2D from the principal conductivity values for an orthotropically aligned benzene crystal assuming that the crystallographic axes of a given material element was determined by the orientation of the interface at the time that material element solidified. They used SL interface shape that they obtained from orthotropic consideration in their calculations and showed that anisotropy is slightly effective only near the ampoule wall. This assumption seems valid only for layers growing parallel to the bottom of the ampoule. They presumed that at sometime during the growth, orientation ( $c$ -axis) changes its direction locally perpendicular to the SL interface, resulting in some degree of polycrystallinity. Their approach is 2D and the results are determined using precalculated SL interface shape for layers growing parallel to the bottom of the ampoule. However, GaSe crystals grown in our laboratory using cylindrical ampoules of various diameters have, most of the times, tendency to grow with  $c$ -axis aligned perpendicular to the ampoule axis and seldom with  $c$ -axis oblique to the ampoule axis. Fig.1 shows such oriented GaSe crystals grown in our Bridgman system. It has also been reported by Anis et al. [16] and Sampaio et al. [17] that their GaSe crystals grew in the same way. Therefore, a conductivity tensor containing only the diagonal elements cannot be used in the simulations of the growth of these crystals if the growth orientation, direction of  $c$ -axis, is different from the ampoule axis.

In this study, a fully anisotropic conductivity tensor that we derived in cylindrical coordinates is used in solving the resultant three dimensional transient heat conduction equation for the growth of a layered crystal GaSe in a cylindrical enclosure by finite difference control volume approximation [18]. The anisotropy in the thermal field is examined for different growth orientations of the crystal with respect to the ampoule axis. Results indicate that the variations of the coefficients of conductivity tensor with the azimuthal angle and growth orientation are quite effective in the resulting thermal field, isotherms and axial and radial temperature gradients. We also investigate the effect of Biot number on the thermal field within the material.

## 2 Anisotropic media

In crystalline or in anisotropic solids, in which certain directions are more favorable for the conduction of heat than others, the component of the heat flux, say  $q_x$  along  $x$ -axis, depends in general on linear combination of the temperature gradients along  $x$ ,  $y$  and  $z$  directions [19]. The general expression for the heat fluxes along the three directions of cartesian system is then given in a compact form as

$$q_i = -\sum_j^3 k_{ij} \frac{\partial T}{\partial x_j} \quad (1)$$

where  $i$  and  $j$  run from 1 to 3, representing  $x$ ,  $y$  and  $z$ -axes. We can therefore state that the flux vector  $q$  is not necessarily normal to an isothermal surface at the point of interest [20].

The thermal conductivity of an anisotropic solid,  $k_{ij}$ , should, therefore, be expressed by a tensor of second rank. Values of the conductivity coefficients depend on the orientation of the reference coordinate system, which is usually a cartesian system since crystals are categorized in cartesian coordinates. This generalized form of conductivity tensor frequently simplifies because of crystalline symmetry if the axes are chosen in appropriate crystallographic directions called principal axes. The principal coordinate system has axes along which the conductivities are the coefficient of a diagonal conductivity tensor.

Most of the layered crystals, such as GaSe, have two principal conductivities; one along the layers and the other is perpendicular to the layers. Hence, the conductivity tensor

$$\tilde{k} = \begin{pmatrix} k_{11} & 0 & 0 \\ 0 & k_{11} & 0 \\ 0 & 0 & k_{33} \end{pmatrix} \quad (2)$$

could be used for the heat conduction problems provided that  $c$ -axis of the crystal is parallel to the  $z$ -axis of the reference coordinate system. This tensor when transformed directly into the cylindrical coordinates preserves its form identically since  $k_{11}=k_{22}$ . These diagonalized tensors are mostly useful only for theoretical investigation of the anisotropic materials in infinite or semi-infinite regions [21]. They may also be used in orthotropic cases where the principal axes of the material line up with the axes of the reference frame describing the thermal process suitable to the boundary of the problem in hand [9,14,15]. However, if the specific problem involves a region surrounded by a finite boundary with an orientation different from the natural orientation of the material, then the conductivity tensor must be transformed into the proper coordinate system that reflects the symmetries of the boundaries. The other alternative is to express the differential equation in canonical form and to transform the boundary conditions in the principal coordinates. The latter method has been applied successfully for an anisotropic medium with a smooth continuous boundary (i.e. spheres, spheroids and ellipsoids) by Mulholand et al. [22]. They were able to reduce a differential equation with mixed derivatives into a simple Laplace's equation by diagonalizing the conductivity tensor. But their method is not proven to be eligible for problems with boundaries which may have sharp edges such as cylinders and cubes. The transformation of the boundary conditions to principle coordinates, in general, can be more complicated than transforming the conductivity tensor from principle coordinates into the coordinates which is appropriate for the boundaries of the thermal process under consideration [23]. In that case the simplicity of the resulting differential equation is sacrificed to accomplish simpler forms of the boundary conditions. But this approach, which is adopted in the present work, is applicable to all types of problems. Therefore, the transformation of the conductivity tensor must be performed using transformation formulae for a physical property expressed by a second rank tensor. Assuming that we need a transformation from coordinate system  $x$ ,  $y$ ,  $z$  to a new coordinate system  $x'$ ,  $y'$ ,  $z'$  suitable to the boundaries under consideration with the direction cosines  $c_{ij}$  relating these two frames, the new conductivity tensor can readily be obtained from the following relation [24];

$$k'_{nm} = \sum_i^3 \sum_j^3 c_m c_{jm} k_{ij}. \quad (3)$$

If the boundary enforces the usage of cylindrical coordinates as in the case of Bridgman crystal growth processes, the transformation of the conductivity tensor must be performed between cartesian and cylindrical coordinate systems.

We derived the following transformation formula for a tensor of second rank between the cartesian and the cylindrical coordinates [18];

$$\kappa_{\sigma\nu} = k_{ij} \left\{ h_\nu \frac{\partial \xi_\nu}{\partial x_j} \right\} \left\{ \frac{1}{h_\sigma} \frac{\partial x_i}{\partial \xi_\sigma} \right\}. \quad (4)$$

The above derivation has been done by the consideration of classical vector analysis outside the tensor theory since we need the physical components in the end [24].

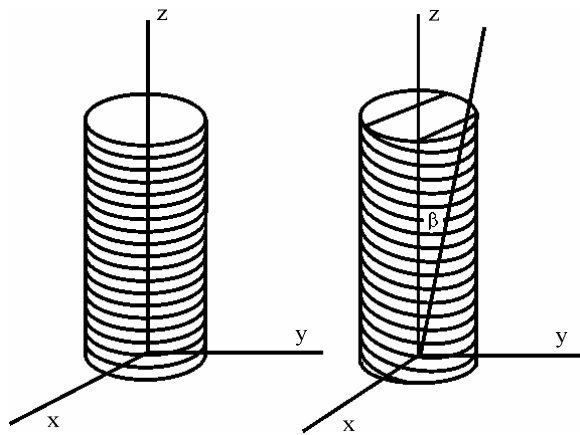


**Fig. 2** Crystallographic orientation of a layered crystal confined in a cylindrical enclosure. a) Orthotropic ( $\beta = 0^\circ$ ), b) Fully anisotropic ( $\beta \neq 0^\circ$ ).

### 3 Application to our system

GaSe crystal that we grow in our laboratory is a layered binary system and has highly anisotropic thermal conductivity. The conductivity in the direction perpendicular to the layer, i.e. along the  $c$ -axis, is  $k_c = k_z = 0.00365$  W/cm $^\circ$ C whereas along the layers  $k_r = 0.0294$  W/cm $^\circ$ C at the melting temperature of GaSe which is 937 $^\circ$ C [14]. Therefore, in a cylindrical growth ampoule, the crystallographic orientation of the solidified portion of the grown material becomes important in the determination of the thermal field which in turn affects the SL interface shape. Figs. 2(a,b) represent schematic diagrams of a layered structure growing in a cylindrical enclosure with  $c$ -axis along  $z$ -axis and along an axis that makes an angle  $\beta$  with  $z$ -axis, respectively. When  $\beta$  is  $0^\circ$ ,  $c \parallel z$ , the layers will be parallel to the bottom of the crucible, then the problem is orthotropic and axially symmetric (Fig. 2a). In this case, the growing layers are perpendicular to the  $z$ -axis so that the conductivity tensors in both cartesian and cylindrical reference systems are diagonal. They can be expressed by second rank tensors in terms of two different conductivity values as the following;

$$\tilde{k} = \begin{pmatrix} k_r & 0 & 0 \\ 0 & k_r & 0 \\ 0 & 0 & k_z \end{pmatrix}. \quad (5)$$

Fig. 2b shows the oblique oriented growth of a layered structure in a cylindrical enclosure with an angle  $\beta$ . When  $\beta \neq 0^\circ$ , the growth should be considered in three dimension since azimuthal symmetry is lifted in such a

case. Hence, one must calculate a conductivity tensor with coefficients depending on the growth orientation angle,  $\beta$ , using Eq. (3) and the direction cosines,  $c_{ij}$ , describing the rotation of the coordinate system by three Euler angles  $\alpha$ ,  $\beta$  and  $\gamma$  for each coordinate.

It is worth mentioning here that  $\beta$  is only important angle, which also determines the growth orientation, since the conductivity tensor of GaSe has two-fold degeneracy, namely, the conduction through the layers is isotropic. That is, the principal conductivities along  $x$  and  $y$ -axes are the same, rotation of the system about  $z$ -axis by an angle  $\alpha$  does not alter the tensor elements. Thus, we applied Euler rotation transformation to the diagonal tensor Eq. (5), to find a new cartesian tensor with nine elements that can be used to construct the heat conduction equation in the rotated rectangular frame coordinates.

With this tensor, we derived the cylindrical conductivity tensor for the problems with cylindrical boundaries using the transformation formula Eq. (4) as:

$$\kappa = \begin{bmatrix} \cos^2(\gamma + \phi)(k_r \cos^2\beta + k_z \sin^2\beta) + k_r \sin^2(\gamma + \phi) & \frac{1}{2}(-k_z + k_r) \sin^2\beta \sin 2(\gamma + \phi) & (-k_z + k_r) \cos\beta \cos(\gamma + \phi) \sin\beta \\ \frac{1}{2}(-k_z + k_r) \sin^2\beta \sin 2(\gamma + \phi) & k_r \cos^2(\gamma + \phi) + (k_r \cos^2\beta + k_z \sin^2\beta) \sin^2(\gamma + \phi) & (k_z - k_r) \cos\beta \sin\beta \sin(\gamma + \phi) \\ (-k_z + k_r) \cos\beta \cos(\gamma + \phi) \sin\beta & (k_z - k_r) \cos\beta \sin\beta \sin(\gamma + \phi) & k_z \cos^2\beta + k_r \sin^2\beta \end{bmatrix} \quad (6)$$

The most of the conductivity coefficients appearing in tensor  $\kappa$  expressed in the cylindrical coordinates have  $\phi$  dependency as expected. Now, the homogeneous medium in cartesian coordinates became heterogeneous in cylindrical coordinates. It should also be pointed out that the rotation angle  $\gamma$  has no significant effect since it can be treated as an offset from the axis where  $\phi$  is measured. The variation of a conductivity coefficient with the azimuthal angle  $\phi$  is evident for an orientation angle  $\beta$  different from zero. Note that for  $\beta=0^\circ$  the  $\phi$  dependency disappears as it should. The  $k_r/k_z$  ratio is about 8.0 for GaSe around its melting temperature. As can be deduced from the cylindrical tensor given above when  $\beta=90^\circ$  conductivity coefficient along the axial direction becomes maximum ( $\kappa_{zz}=k_r$ ) where layers are aligned parallel to the  $z$ -axis. At that angle  $\kappa_{zz}$  and/or  $\kappa_{rz}$  disappears leaving  $\kappa_{zz}$  as the only important parameter in terms of the heat transfer along axial direction. This will be the case for any layered semiconductor.

It must be emphasized that the cylindrical tensor, Eq. (6), obeys, as it should, the Onsager's rules of irreversible processes of thermodynamics [25]. This is expected because the physics of a process must be invariant under the coordinate transformation.

The heat fluxes when transformed into cylindrical coordinates for an obliquely oriented anisotropic crystal are as the following;

$$q_\mu = - \sum_{\nu}^3 \kappa_{\mu\nu} \frac{1}{h_\nu} \frac{\partial T}{\partial \xi_\nu} \quad (7)$$

where  $\mu$  and  $\nu$  run from 1 to 3, representing  $r$ ,  $\phi$  and  $z$ -axes.

Using the above equations for the heat fluxes along each direction in cylindrical coordinates, in the time dependent heat conduction equation  $-\vec{\nabla}_\xi \cdot \vec{q} = \rho c_p \frac{\partial T(r, \phi, z, t)}{\partial t}$ , we derived the differential equation;

$$\begin{aligned} & \kappa_{rr} \frac{\partial^2 T(r, \phi, z, t)}{\partial r^2} + \kappa_{rr}' \frac{1}{r} \frac{\partial T(r, \phi, z, t)}{\partial r} + \kappa_{\phi\phi} \frac{1}{r^2} \frac{\partial^2 T(r, \phi, z, t)}{\partial \phi^2} + \kappa_{zz} \frac{\partial^2 T(r, \phi, z, t)}{\partial z^2} + 2\kappa_{r\phi} \frac{1}{r} \frac{\partial^2 T(r, \phi, z, t)}{\partial r \partial \phi} + 2\kappa_{rz} \frac{\partial^2 T(r, \phi, z, t)}{\partial r \partial z} \quad (8) \\ & + 2\kappa_{z\phi} \frac{1}{r} \frac{\partial^2 T(r, \phi, z, t)}{\partial z \partial \phi} + (\kappa_{z\phi}' + \kappa_{rz}) \frac{1}{r} \frac{\partial T(r, \phi, z, t)}{\partial z} + \kappa_{r\phi}' \frac{1}{r} \frac{\partial T(r, \phi, z, t)}{\partial r} + \kappa_{\phi\phi}' \frac{1}{r^2} \frac{\partial T(r, \phi, z, t)}{\partial \phi} = \rho c_p \frac{\partial T(r, \phi, z, t)}{\partial t} \end{aligned}$$

where  $\kappa'_{\mu\nu}$  represents the derivatives of  $\kappa_{\mu\nu}$  with respect to azimuthal angle  $\phi$ . Since the determinant of the conductivity tensor is positive the resulting differential equation of heat conduction is of the elliptic type for steady state and of the parabolic type for the unsteady state.

Although derived for two-fold degenerate orthorhombic system with hexagonal symmetry, the above equation seems quite complicated to solve. It would be worse for other crystallographic systems especially in spherical coordinates. Because of the presence of the variable coefficients and the mixed derivatives in Eq. (8) analytical or numerical solution is rather difficult to obtain compared to isotropic counterparts [21]. That is, maybe, why no solution is available in the literature for this equation. Similar equations with constant coefficients for homogeneous media in the cylindrical coordinates (that is not physically possible because of the curved nature of the cylindrical coordinates) have been solved analytically by Chang et al. [27,28] and Ozisik et al. [29].

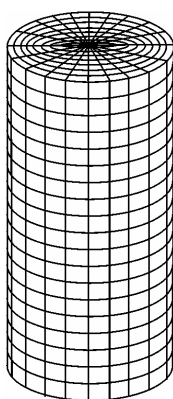


**Fig. 3** Simplified diagram of the control volume elements used in numerical procedure.

**Table 1** Physical parameters used in the numerical simulation.

Parameter	Value	Unit
$k_a$	0.0026	$\text{W mm}^{-1}\text{K}^{-1}$
$k_r$	0.00293	$\text{W mm}^{-1}\text{K}^{-1}$
$k_z$	0.000365	$\text{W mm}^{-1}\text{K}^{-1}$
$c_{p_s}$	1.25	$\text{J g}^{-1}\text{K}^{-1}$
$c_{p_l}$	0.34	$\text{J g}^{-1}\text{K}^{-1}$
$\rho_a$	2.2	$\text{g cm}^{-3}$
$\rho_s$	4.93	$\text{g cm}^{-3}$
$L$	50.0	$\text{mm}$
$r_o$	.0	$\text{mm}$
$d$	2.0	$\text{mm}$

#### 4 Numerical solution

Our goal in the present study is to investigate the effect of anisotropic thermal conductivity on the formation of the thermal field during the growth of GaSe or similar crystals enclosed in cylindrical ampoules. For the purpose we developed a computer code that makes use of the implicit finite difference approximation of the Eq. (8) for the solidified portion. Because the inclusion of the interface between the solid and the melt brings along an extra complication to the computational procedure it is not considered in this paper. Hence we assume that all material in the ampoule is solid. With this assumption we will be able to investigate the thermal field in growth processes when solidified fraction dominates.

The lack of azimuthal symmetry causes the Eq. (8) to have a singular point at  $r=0$  and makes it inconvenient for numerical works. On the other hand, with the aid of control volume formalism the singularity is prevented and the physical picture becomes more visible through which we can decide what difference scheme to apply. Since the grown material is put in a growth ampoule that is pulled down in a three zone vertical Bridgman system, our model includes a cylindrical ampoule with a varying temperature profile with

respect to time along its lateral surface. Within the ampoule, 3D isotropic heat conduction equation must also be used since the ampoule encloses an anisotropic medium. In obtaining the solution to the equation S.O.R. iterative technique is employed because a convergent A.D.I. scheme is very difficult to find [30]. The simulation domain is constructed with 72 nodal points in  $\phi$  direction with the nodes placed at the center of the volume elements. The number of nodal points is 24 and 108 in  $r$  and  $z$  directions, respectively. A simplified diagram of grid configuration is shown in Fig. 3. Thus, the total number of control volume elements used in the simulation is 186,624.

The external boundary conditions are chosen to reflect actual situation in Bridgman growth. The Newton's cooling law was applied between the ampoule walls and the environment, namely,

$$\begin{aligned} \text{at } r = r_o + d : \quad & -q_r^+ = h(T_a(z) - T(r = r_o + d, \phi, z)) \\ \text{at } z = 0 : \quad & +q_z^- = h(T_a(z = 0) - T(r, \phi, z = 0)) \\ \text{at } z = L + 2d : \quad & -q_z^+ = h(T_a(z = L + 2d) - T(r, \phi, z = L + 2d)) \end{aligned}$$

where  $h$  is heat transfer coefficient, which is same for all boundaries and  $T_a$  is the ambient temperature distribution and we assumed it to vary linearly as  $T_a(z) = 1200.0 - 2.0 z$  [ $^{\circ}\text{C}$ ],  $z$  in  $mm$ , based on the measured temperature profile along the furnace axis near the melting temperature of GaSe. (For convenience  $z$ -axis is chosen downwards, which is in the opposite direction of the conventional  $z$ -axis.)

Equations and the boundary conditions are non-dimensionalized by defining a dimensionless temperature as  $\theta = (T - T_m) / \Delta T$  where  $T_m$  is  $937^{\circ}\text{C}$  and  $\Delta T = 600^{\circ}\text{C}$ . The dimensionless coordinates are defined as  $R = r / r_o$  and  $Z = z / r_o$  where  $r_o$  is the inner radius of the ampoule. The time is non-dimensionalized by:  $\tau = \frac{t k_a}{r_o^2 \rho_a c_p}$

The simulation is started by assigning the ambient temperature profile to all grid points of corresponding height at the hot zone of the furnace. The steady-state solution is obtained at that position and then the crucible is moved down in the direction of decreasing temperature. During this period a number of snap shuts are taken to monitor the process.

## 5 Results and discussion

The thermal field in an anisotropic solid enclosed in an ampoule with isotropic properties has been investigated for various crystallographic orientations. The Biot number (Bi), which is a measure of the rate of heat exchange between the furnace and the ampoule wall, was set to the values 0.1, 0.5, 1.0 and 1.5. We used the principal conductivity ratio of GaSe as  $k_r / k_z = 8.0$  at its melting temperature  $T_m = 937^{\circ}\text{C}$ . Table 1 gives the input parameters used in the simulation.

In order to test our model and the computer program, we firstly run it for  $k_r / k_z = 1.0$ , and the resulting thermal field that we obtained for any growth orientation angle was axially symmetric, agreeing with our and the other 2D isotropic numerical solutions.

We analyzed the thermal fields on a cross sectional plane at the top, the bottom and the central regions of the material for different growth orientation angles,  $\beta$ . The steady state solution for  $\beta = 0^{\circ}$  results in a constant temperature at the central region as expected since the applied ambient temperature profile is linear. For  $\beta = 90^{\circ}$ , we were expecting considerable  $\phi$  dependence because at this angle the non-vanished conductivity coefficients other than  $\kappa_{zz}$  varies wildly with  $\phi$ . However, we observed a very weak variation of the temperature with a maximum temperature difference of around 0.02K over the cross-sectional plane at the half length of the material. It is difficult to explain this behavior by means of mathematical consideration, but it can be explained by visualizing the layers as highly conductive sheets lining up with  $z$ -axis and having rectangular shapes with the sides touching to the ampoule wall. Then every single sheet separated by low conductive layers will have the same boundary conditions at the periphery viewed in two dimension. Therefore, the relaxation of the

thermal field is achieved due to high conductivity along the layers symmetrically distributed across all the points at the periphery. At the top and the bottom,  $\phi$  dependence of the thermal field becomes more pronounced reaching a maximum temperature difference of 3.0K. This is due to the  $\phi$  dependence of the end effects because of the high anisotropy.

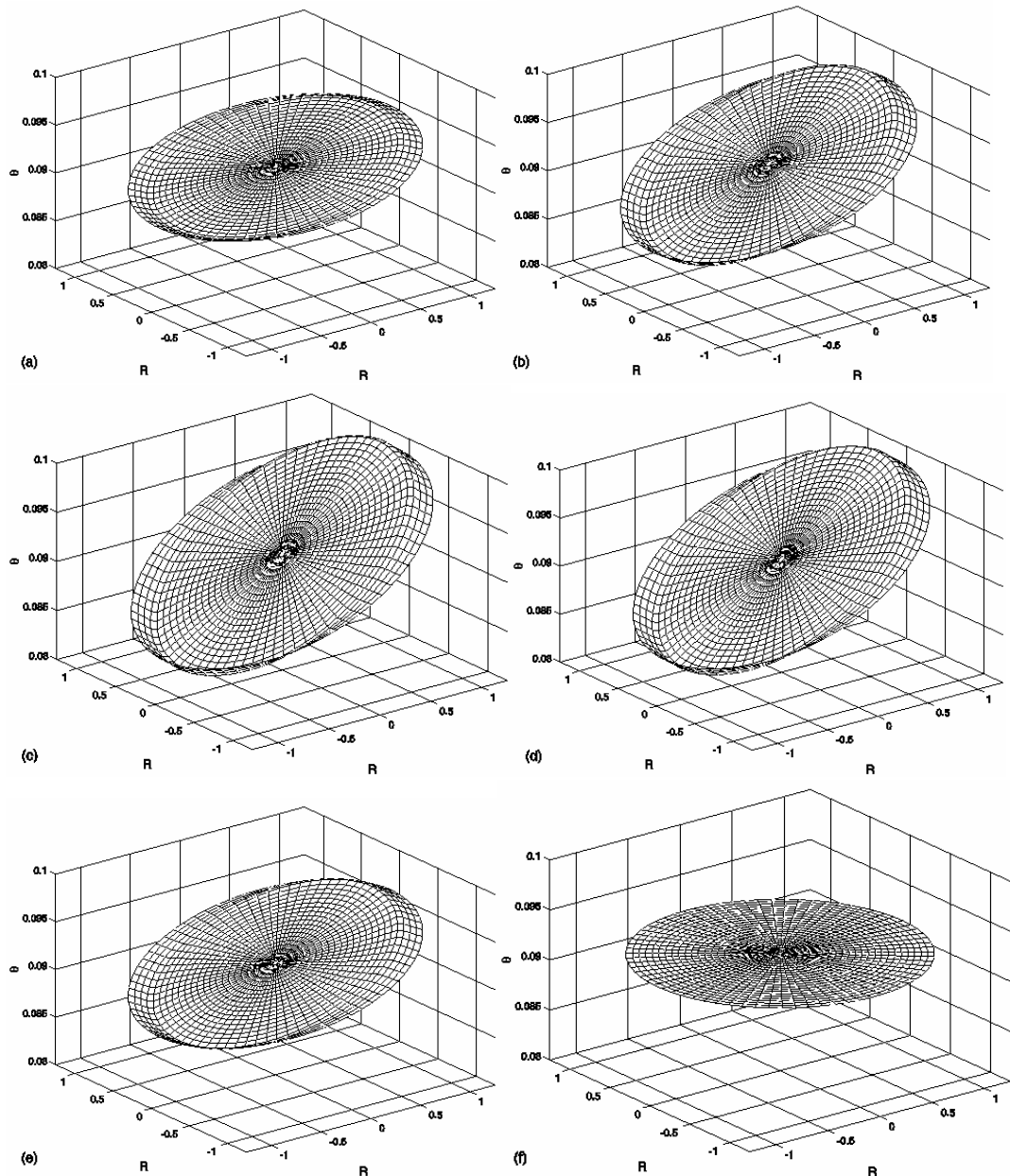


**Fig. 4** Temperature distribution over the plane at  $z=L/2+d$  obtained for different growth orientation angles. a)  $\beta=15^\circ$ , b)  $\beta=30^\circ$ , c)  $\beta=45^\circ$ , d)  $\beta=60^\circ$ , e)  $\beta=75^\circ$ , f)  $\beta=90^\circ$ .

Figs. 4(a-f) are the representations of thermal fields taken on a plane with a circular cross section at  $z=L/2+d$ , for a stationary crucible for  $Bi=1.0$ . As mentioned above, the temperature is  $\phi$  independent for the growth angle  $\beta=90^\circ$  (Fig. 4f). When the growth angle is in between  $0^\circ$  and  $90^\circ$  temperature varies with the azimuthal angle,  $\phi$ , as indicated in these figures. This temperature variation with respect to  $\phi$  becomes maximum for  $\beta=45^\circ$  (Fig.

4c), reaching a temperature difference of around 15K on the cross sectional plane within the cylindrical ampoule. Similarly, isothermal surfaces have strong  $\phi$  dependence as the thermal field which, certainly, cannot be observed for isotropic and orthotropic cases. To present the variation of isothermal lines with azimuthal angle,  $\phi$ , we give two dimensional contour plots drawn on  $r$ - $z$  plane for different  $\phi$  values in Figs. 5(a-f), for the growth orientation of  $\beta=45^\circ$ . One can observe the variation of the slope of the isothermal lines on the isothermal surface for different azimuthal angles from Fig. 5 plotted for  $\phi = (0,180), (15,195), (45,225), (60,240), (75,225), (90,270)$ .

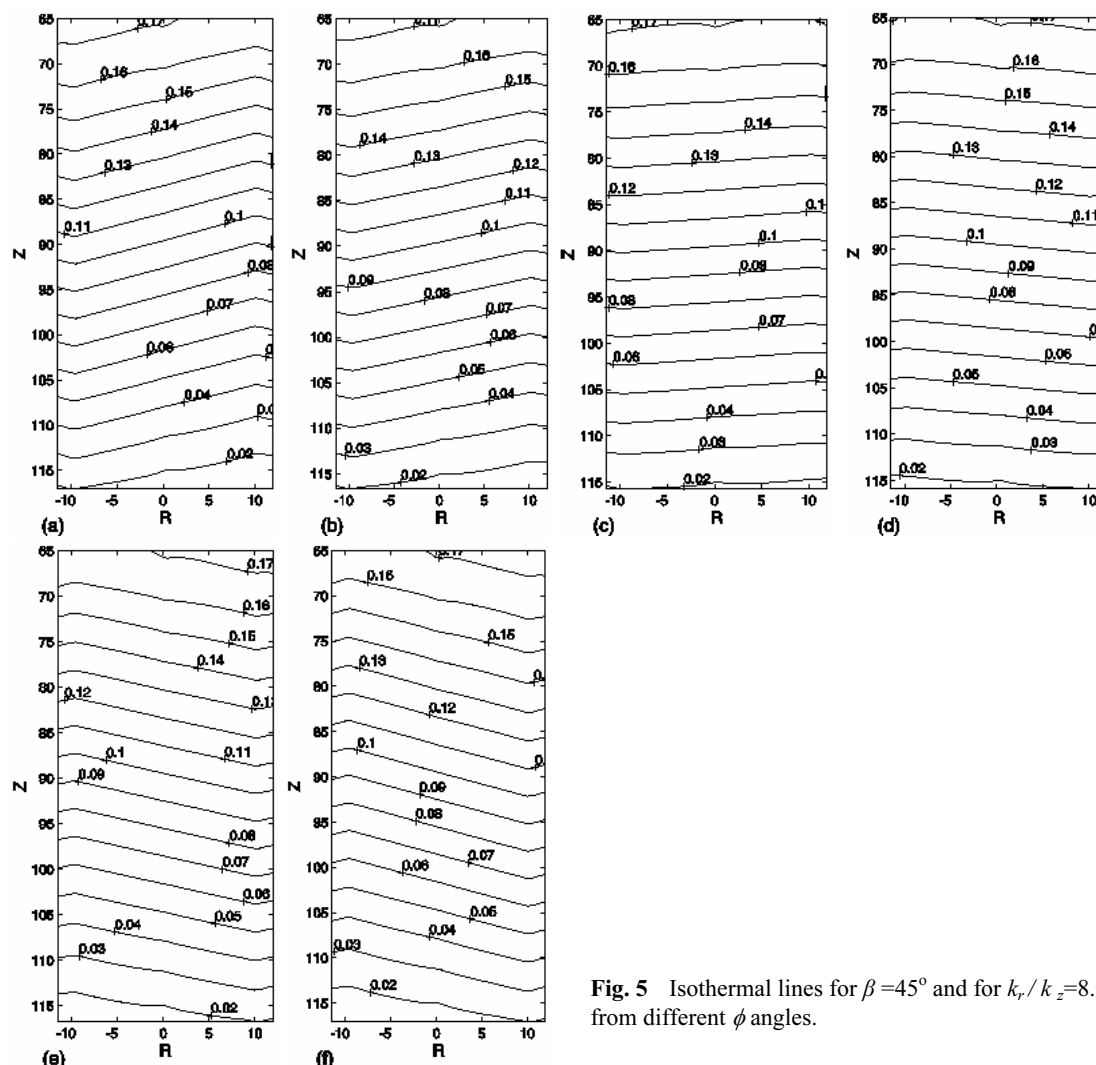


Fig. 5 Isothermal lines for  $\beta=45^\circ$  and for  $k_r/k_z=8.0$  viewed from different  $\phi$  angles.

In Fig. 6 the slopes of the isothermal surfaces are plotted as functions of growth orientation,  $\beta$  and Bi number for the thermal conductivity ratio,  $k_r/k_z=8.0$ . The slope of an isothermal surface is defined here as the angle between the isothermal surface and the horizontal  $r - \phi$  plane. As can be seen from the figure the slopes of the isothermal surfaces increases as the growth orientation  $\beta$  increases up to  $\beta=45^\circ$  at where it reaches a maximum value. The reason is that at this growth orientation, the effect of off-diagonal conductivity coefficients,  $\kappa_{rz}$  and  $\kappa_{\phi z}$  is maximized. This effect is reduced reaching a relaxation of the thermal field, resulting a horizontal isothermal surface at  $\beta=90^\circ$ . Such variation of the slopes of isothermal surfaces with  $\beta$  also affects the heat transfer rates between the material sides and the inner periphery of the ampoule which, in principle, controls the thermal stresses at the boundary during the growth of the crystal.

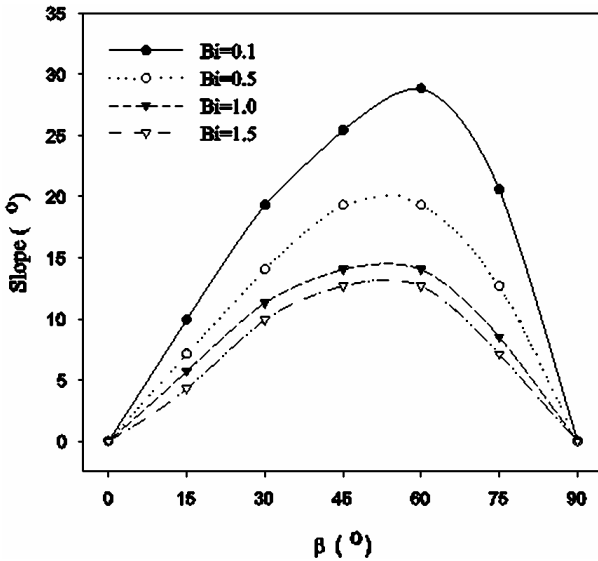


Fig. 6 Variation of the angle between the horizontal plane and the isothermal surfaces w.r.t. orientation angle,  $\beta$ , for different Bi numbers, ( $k_r/k_z=8.0$ ).

The Bi number has also been found to be effective on the slope of the isothermal surfaces, especially for Bi values between 1.0 to 0.1, which is the range in the real growth processes for quartz ampoule calculated with  $h$  values proposed in [31,32]. The magnitude of the slope is inversely proportional to the Bi number as indicated in the figure. This can be explained by the increase of the heat transfer rates between the ampoule outer wall and the environment as Bi is increased, which in turn affects the heat transfer rates between the ampoule inner wall and the material. This increase in the rates enforces the isothermal surfaces toward smaller slopes so that the thermal field within the material approaches to the  $\phi$  independent temperature profile applied at the boundary. As Bi is decreased, the conductivity anisotropy within the material becomes more effective than Newton's Cooling on the resulting thermal field and thus producing isothermal surfaces having higher slopes.

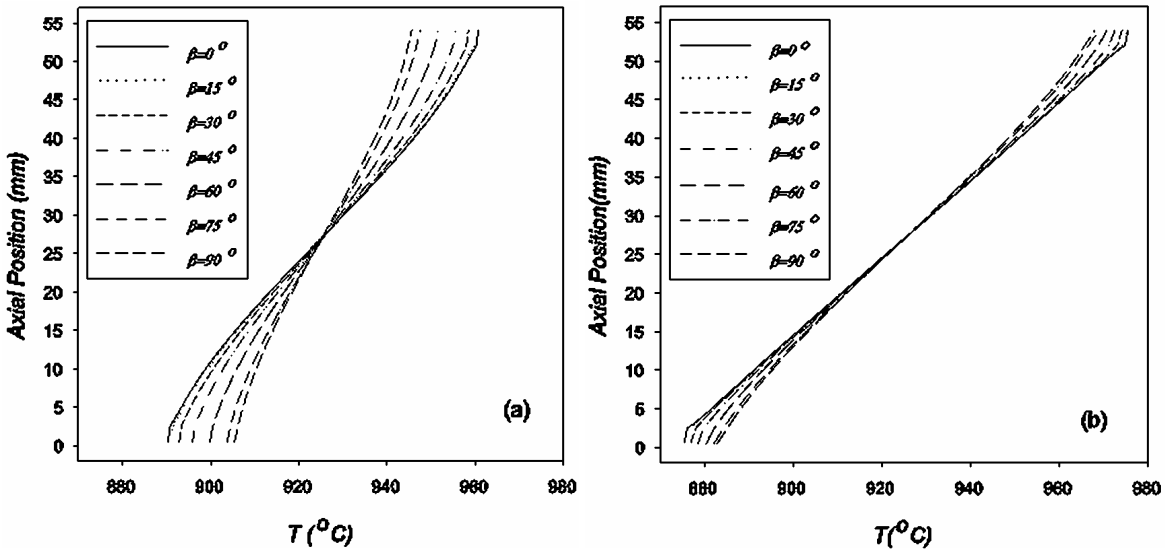


Fig. 7 The axial temperature variations with respect to  $\beta$  along the center of the stationary ampoule for  $k_r/k_z=8.0$ . a)  $Bi=0.1$ , b)  $Bi=1.0$ .

We investigated the temperature variation along the  $z$ -axis for  $k_r/k_z=8.0$  and  $Bi=1.0$  and  $0.1$  for different growth orientations. As shown in Fig. 7a, changing  $\beta$  from  $0^\circ$  to  $90^\circ$  decreases the temperature difference about

20°C between the top and the bottom of the ampoule giving rise to a more relaxed thermal field. This reduced gradient means that the conduction becomes more effective in axial direction so that the gradient imposed by the applied temperature profile is well-transferred through the material. Another beneficial effect of increased conduction in the axial direction would have been observed on the SL interface when  $k_l / k_s$  ratio becomes smaller by increasing  $\beta$ . Then the heat generated via phase change would be conducted better through the solid to the bottom of the ampoule resulting a relatively flatter interface [33].

The effect of the Bi number on the axial gradient can be deduced from the comparison of Figs. 7a and 7b. We observed that decreasing the Bi number results in a reduction of the axial temperature gradient which is far below the imposed temperature profile at the boundary (Fig. 7a). For Bi=1.0 (Fig. 7b) and above, axial temperature distribution begins to maintain the furnace temperature profile with a gradient of  $2.0\text{K mm}^{-1}$  within the material.

The thermal fields for non-stationary ampoule travelling with different constant velocities have been examined. We observed that the increase in the velocity from  $50.0\text{ mm/h}$  to  $300\text{ mm/h}$  causes an increase in the deflection (concavity) of the isothermal surface from  $1.0\text{ mm}$  to  $1.75\text{ mm}$  for the ampoule radius of  $1.0\text{ cm}$  that we used in the simulations and for  $\beta=90^\circ$  growth orientation. The same effect is observed for all the growth orientation with an increasing concavity over the oblique isothermal surfaces as the pulling rate is increased, the magnitude of which are almost the same as in  $\beta=90^\circ$  case. The position of isothermal surface and the amount of concavity are slightly dependent on the angle  $\beta$  for travelling ampoule. The radial thermal gradient also increases with increasing velocity. Asymmetry in radial temperature gradient due to anisotropy can be observed, which is important in actual growth processes.

## 6 Conclusion

In the control of the SL interface shape and the position, the ratio  $k_l / k_s$  known to be one of the most important factors. When anisotropic crystals are grown, instead of  $k_s$ , one needs to use an effective solid conductivity at the SL interface, then this ratio will be dependent on the crystallographic orientation of the crystal in the growth ampoule. The heat exchange between the furnace and the material will also be dependent on the conductivity coefficients due to the dependence of the effective Bi number on the coupling between the solid and the ampoule conductivities [11].

One of the most important conditions to grow better crystals using melt growth techniques is that the heat flowing in the crystal away from the SL interface must be greater than the rate of latent heat evolution, [6]. This results in a flatter SL interface shape. For layered crystals as GaSe,  $\beta=90^\circ$  growth orientation satisfies this condition since at this orientation the conductivity perpendicular to the isothermal surface (i.e. along the  $z$ -axis) is maximized. This analysis may explain why our most successful growths in our laboratory happen to have  $\beta=90^\circ$  growth orientation.

The consideration of full anisotropy in numerical simulations will extend our predictions of the best growth conditions. Traditional growth techniques may also be modified for the growth of such materials. At least the choice of the ampoule material and the shape should be considered accordingly.

**Acknowledgements** This work was financially supported by METU-AFP under the project contract number AFP-2001-01-07-02-00-013. The authors would like to thank to Dr. O. Karabulut for his helps.

## Nomenclature

### Greek

- $\alpha, \beta, \gamma$  rotation angles about  $z, x'$  and  $z''$ .  
 $\theta$  dimensionless temperature.  
 $\kappa$  conductivity tensor in curvilinear coordinates.

$\kappa_{\mu\nu}$	conductivity coefficients in curvilinear coordinates.
$\xi_{\mu}$	axes in curvilinear coordinates.
$\rho_a, \rho_s$	density of the ampoule and the solid.
$\tau$	dimensionless time.
$\phi$	azimuthal angle in the cylindrical coordinates.
$\vec{\nabla}_{\xi}$	divergence operator in cylindrical coordinates.

### Latin

Bi	Biot number.
$c_{ij}$	direction cosines of Euler coordinate rotations.
$c_{P_a}, c_{P_s}$	specific heat of ampoule and solid.
d	thickness of ampoule.
h	heat transfer coefficient.
$h_{\mu}$	scale factors for cylindrical coordinates.
k	conductivity tensor in cartesian coordinates.
$k_a, k_l, k_s$	thermal conductivity coefficients of ampoule, liquid and solid.
$k_{ij}$	conductivity coefficients in cartesian coordinates.
$k_r$	conductivity of solid along x-y plane of principle coordinates.
$k_z$	conductivity of solid along z-axis of principle coordinates.
L	length of solid.
$q_i$	heat flux components in cartesian coordinates.
$q_{\mu}$	heat flux components in cylindrical coordinates.
$r_o$	inner radius of ampoule.
r, z	axes in cylindrical coordinates.
R, Z	dimensionless form of the axes r and z.
t	time.
T	temperature.
$T_a$	ambient temperature.
$T_m$	melting temperature.
$x_i$	axes in cartesian coordinates.

### References

- [1] B. R. Pamplin, *Crystal Growth* (Pergamon Press, N.Y. 1975).
- [2] J. Czochralski, *Z. Phys. Chem.* **92**, 219 (1918).
- [3] W. G. Pfann, *Trans. A.I.M.E.* **194**, 747 (1952).
- [4] P. W. Bridgman, *Proc. Amer. Acad. Arts. Sci.* **60**, 305 (1925).
- [5] E. C. Chang and W. R. Wilcox, *J. Cryst. Growth* **21**, 135 (1974).
- [6] J. C. Brice, *Crystal Growth Processes* (John Wiley and Sons, N.Y. 1986).
- [7] T. W. Fu and W. R. Wilcox, *J. Cryst. Growth* **48**, 416 (1980).
- [8] R. Feigelson and R. K. Route, *J. Cryst. Growth* **49**, 261 (1980).
- [9] C. E. Huang, D. Elwell, and R. S. Feigelson, *J. Cryst. Growth* **64**, 441 (1983).
- [10] J. L. Plaza and E. Dieguez, *Cryst. Res. Technol.* **36**, 695 (2001).
- [11] T. Jasinski, W. M. Rohsenow, and A. F. Witt, *J. Cryst. Growth* **61**, 339 (1983).
- [12] C. Barat, T. Duffar, and J. P. Grandet, *J. Cryst. Growth* **194**, 149 (1998).

- [13] D. H. Kim and R. A. Brown, *J. Cryst. Growth* **96**, 609 (1989).
- [14] H. Lee and A. J. Pearlstein, *J. Heat Transfer* **123**, 729 (2001).
- [15] H. Lee and A. J. Pearlstein, *J. Cryst. Growth* **209**, 934 (2000).
- [16] M. K. Anis, *J. Cryst. Growth* **55**, 465 (1981).
- [17] H. Sampaio, A. Gousov, and Z. P. Arguello, *J. Cryst. Growth* **41**, 275 (1977).
- [18] E. Tasarkuyu. Ph.D. Thesis, Department of Physics, METU, Ankara, Turkey, (2003).
- [19] H. S. Carslaw and J. C. Jaeger, *Conduction of Heat in Solids* (Oxford University Press, London, 1959).
- [20] M. N. Ozisik, *Heat Transfer-A Basic Approach* (McGraw-Hill Co., N.Y., 1985).
- [21] Y. P. Chang, *Int. J. Heat Mass Transfer* **20**, 1019 (1977).
- [22] G. P. Mulholland and B.P. Gupta, *J. Heat Trans.* **99**, 135 (1977).
- [23] Y. P. Chang, C. S. Kang, and D. J. Chen, *Int. J. Heat Mass Transfer* **16**, 1905 (1973).
- [24] E. Butkov, *Mathematical Physics* (Addison-Wesley Publishing Company, Reading, Massachusetts, 1968).
- [25] L. Onsager, *Phys. Rev.* **37**, 405 (1931).
- [26] T. Jasinski and A. F. Witt, *J. Cryst. Growth* **71**, 295 (1985).
- [27] Y. P. Chang and R. C. H. Tsou, *J. Heat Trans.* **99**, 132 (1977).
- [28] Y. P. Chang and R. C. H. Tsou, *J. Heat Trans.* **99**, 41 (1977).
- [29] M. N. Ozisik and S. M. Shouman, *J. The Franklin Institute* **309**, 457 (1980).
- [30] A. R. Gourley and S. McKee, *J. Comp. Appl. Math.* **3**, 201 (1977).
- [31] W. Rosch, W. Jesser, W. Debnam, A. Fripp, G. Woodell, and T. K. Pendergrass, *J. Cryst. Growth* **128**, 1187 (1993).
- [32] W. Rosch, A. L. Fripp, W.J. Debnam, and T.K. Pendergrass, *J. Cryst. Growth* **174**, 139 (1997).
- [33] D. H. Kim, R. A. Brown, *J. Cryst. Growth* **109**, 66 (1991).